J|A|C|S COMMUNICATIONS

Published on Web 07/02/2009

Electrochemical Gate-Controlled Charge Transport in Graphene in Ionic Liquid and Aqueous Solution

Fang Chen,[†] Quan Qing,[‡] Jilin Xia,[†] Jinghong Li,[§] and Nongjian Tao*,[†]

Center for Bioelectronics and Biosensors, Biodesign Institute, Department of Electrical Engineering, Arizona State University, Tempe, Arizona 85287, Department of Chemistry and Chemical Biology, Harvard University, Cambridge, Massachusetts 02143, and Department of Chemistry, Tsinghua University, Beijing 100084, China

Received May 22, 2009; E-mail: nongjian.tao@asu.edu

Graphene is a sheet of sp^2 bonded carbon atoms that are arranged into a honeycomb structure.[1,2] This two-dimensional material has many unique properties,[3] which promise important electronic device applications.[4,5] Because of the single-atom thickness, the charge transport properties of graphene are extremely sensitive to its local environment, thus making it particularly attractive for sensor applications.[6] Schedin et al.[7] have reported the detection of a single gas molecule with a graphene field effect transistor (FET). Ang et al.[8] have shown that graphene electrical properties are sensitive to pH. However, biosensor applications require operating the device at or near physiological conditions, so it is critical to study graphene in aqueous solutions and to understand the interactions of ions with graphene. Using a back gate controlled graphene FET, we have recently shown that ions can have a profound effect on the electron transport properties of the graphene FET via screening of impurity charges in the device.[9,10]

In the present work, we study the charge transport in electrochemically gated graphene under different electrolytes, including ionic liquids and aqueous solutions. In addition to the direct relevance to biosensors, the electrochemical gate is also expected to be much more effective than the back gate approach in tuning the charge carriers. This is because the applied gate voltage in electrochemically gated FETs falls across the double layer formed at the graphene−solution interface. The double layer thickness is determined by the size of the ions (~1 nm), which is several orders of magnitude thinner than that of oxide (~300 nm) used in a back gate configuration. In an ionic liquid, we are able to determine the mobile carrier density using a simplified capacitor model and interpret the electron transport characteristics in terms of charged impurity induced scattering. In aqueous solutions, we find a systematic dependence of the conductivity shift on the ionic concentration and model the dependence in terms of surface potential that is determined by the impurity charges on the SiO_2 substrate and distribution of ions in bulk solution.

Single layer graphene was exfoliated from Kish graphite (Figure 1b, inset), and we have verified the thickness of the graphene layer using an optical micrograph and a Raman spectrum (Supporting Information). Ti is used as source and drain electrodes to minimize the leakage current from ions to metal because of the presence of native oxide on the Ti surface. Figure 1b shows a typical conductivity vs electrochemical gate potential plot obtained in an ionic liquid, 1-butyl-3-methylimidazolium hexafluorophosphate ($BmimPF_6$). Details for the synthesis of $BmimPF_6$ have been published.[11] The conductivity reaches a minimum value at the charge neutral point and linearly increases with the gate potential on both sides. In the ionic liquid, due to the high ionic concentration of $BmimPF_6$ (~6 M), the thickness of the diffuse layer is negligible,[12] which has been used to provide effective gating for electron transfer in redox molecules.[13]

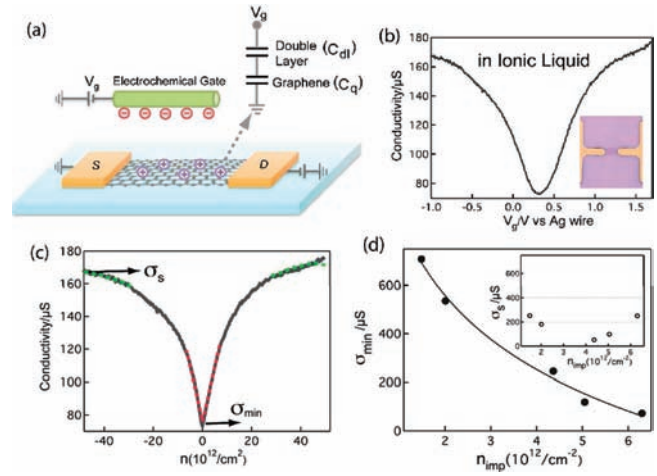

Figure 1. (a) Schematic diagram of electrochemical gate tuned graphene FET devices. Inset is the graphene−solution interface capacitance model. (b) Transport characteristic of graphene FET that is conducted in ionic liquid (1-butyl-3-methylimidazolium hexafluorophosphate). Inset: optical micrograph of a graphene transistor. (c) Conductivity vs carrier density trace corresponding to (a). (d) Dependence of minimum conductivity σ_{min} and plateau conductivity σ_s on the concentration of charged impurities.

Since the diffuse layer capacitance is negligible, the interfacial capacitance can be modeled as two capacitors in series, one due to the ionic double layer, C_{dl}, and the other being of quantum origin, C_q (Figure 1a, inset). C_{dl} in $BmimPF_6$ is ~20 μF/cm^2, which is insensitive to the gate potential and in quantitative agreement with the literature.[14] The potential independent double layer capacitance has been studied and reported elsewhere.[15] C_q is a function of carrier density or gate voltage.[16] The potential dropped on the two capacitors is then given by[17]

$$\left|V_g - V_{g,min}\right| = \frac{h \cdot v_F \cdot \sqrt{\pi n}}{e} + \frac{ne}{C_{dl}}$$

where h is the reduced Planck's constant, v_F is the Fermi velocity of the Dirac electron in graphene, e is the electron charge, and n is the carrier density. Using this relation, V_g is converted to n, and the measured conductivity (σ) vs n is plotted in Figure 1c. The trace reveals a sharp conductivity minimum at zero n and increases dramatically outside the minimum due to the high electron/hole density induced by the gate potential. From the slope of linear regimes (red dashed lines in Figure 1c), we can calculate the carrier mobility using $\mu = (d\sigma/dn)/e$.

As an example, the hole mobility is found to be ~1200 cm^2/v·s for the device shown in Figure 1b. At high n, the conductivity begins

[†] Arizona State University.
[‡] Harvard University.
[§] Tsinghua University.

10.1021/ja9041862 CCC: $40.75

to saturate (green dashed lines in Figure 1c) and approaches a plateau value eventually. This behavior has been attributed to the carrier scattering by the atomic defects or ripples in graphene,[18] and it was observed in back gated graphene FETs[17] but required fairly large gate voltages. In contrast, the electrochemical gate configuration allows one to control the carrier density over a much wider range, making it an efficient way to study different scattering mechanisms by the same device, which is an important task in the study of graphene electronics.

It is well established that the transport at low n is dominated by the impurity charges underneath graphene, which leads to long-range Coulomb scattering of the carriers. By fitting the conductivity vs n data collected from five different devices with the theory,[19] we have estimated the concentration of charged impurities in each device, n_{imp}, varying from $\sim 10^{12}$ to $\sim 10^{13}$ cm^{-2} (Figure 1d), which is consistent with other reports.[18] At zero carrier density, the conductivity is not zero, which also suggests the presence of charged impurities. We plot the minimum conductivity σ_{min} vs n_{imp} (Figure 1d) and find that σ_{min} decreases rapidly with n_{imp}. In other words, under the circumstance of zero induced carriers, clean samples are more conductive than dirty ones as predicated by the Coulomb scattering theory.[19] In contrast, the plateau conductivity, σ_s, does not show obvious dependence on n_{imp} (Figure 1d, inset) among different batches of devices. This is also anticipated because the counterions accumulated on the graphene surface do not modify the atomic potential of crystal defects or ripples.[9]

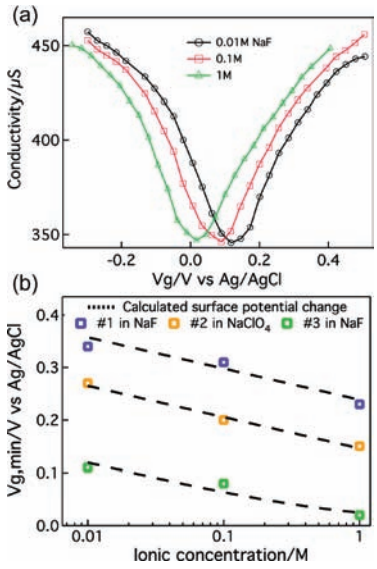

Figure 2. (a) Conductivity comparison in aqueous solution containing different concentrations of NaF (0.01, 0.1, and 1M, respectively). (b) The conductivity shift measured in NaF (purple and orange squares) and in $NaClO_4$ (green squares) compared to the calculated surface potential change (dotted line) as a function of ionic concentration.

Figure 2a illustrates the conductivity of the same device measured at different NaF concentrations, ranging from 0.01 to 1 M. The most profound change is that the position of the conductivity minimum shifts toward negative potentials with the ionic concentration and reaches nearly zero at high concentrations (Figure 2a, green curve). The shift in the conductivity minimum is reversible (Figure s1), which excludes the carrier doping origin of the ionic concentration dependency. We repeat the measurement in $NaClO_4$ and observe similar changes. Na^+, F^-, and ClO_4^- ions are chemically inert and do not specifically adsorb on the graphite surface.[20] We believe that the ionic concentration dependency is due to the screening of the impurity charges by the ions in solution phase.[9]

The surface of the SiO_2 associated surface potential depends on the ionic concentration given by[21]

$$\psi_s = \frac{2kT}{e} \sinh^{-1}\left(\frac{e\alpha}{\sqrt{8\varepsilon\varepsilon_0 kT 1000 N_A[c]}}\right)$$

where α is the density of surface charge and is the surface potential. By substituting different values of charge density, i.e., 1.3×10^{12} cm^{-2}, the data of device #3 shown in Figure 2b (green) can be fitted (dotted line). Likewise, we fit the data of devices #1 and #2 via adopting 22×10^{12} and 50×10^{12} cm^{-2}, respectively. It should be noted that α here is not equal to n_{imp} because the mobile carriers in graphene can partially screen the impurity charges, but the two quantities are correlated.[19] This simple model explains the dependence of graphene transport characteristics on ionic concentration.

In summary, we have applied an electrochemical-gating approach to study the charge transport in single layer graphene transistors in ionic liquids and aqueous solutions. In an ionic liquid, we determined the carrier density as a function of electrochemical gate potential and estimated the concentration of charged impurities, as well as other related transport quantities. While under aqueous solutions, the position of the minimum conductivity shifts toward lower potentials as the ionic concentration increases, and this shift has been modeled in terms of impurity charge induced surface potential change, which is sensitive to the ionic concentration.

Acknowledgment. We thank NSF (CHE-0554786, F.C.) and DOE (DE-FG03-01ER45943, J.X.) for financial support.

Supporting Information Available: Experimental details, data fitting, and more plots are provided. This material is available free of charge via the Internet at http://pubs.acs.org.

References

(1) Stolyarova, E.; Rim, K. T.; Ryu, S. M.; Maultzsch, J.; Kim, P.; Brus, L. E.; Heinz, T. F.; Hybertsen, M. S.; Flynn, G. W. *Proc. Natl. Acad. Sci. U.S.A.* **2007**, *104*, 9209.
(2) Ishigami, M.; Chen, J. H.; Cullen, W. G.; Fuhrer, M. S.; Williams, E. D. *Nano Lett.* **2007**, *7*, 1643.
(3) Geim, A. K.; Novoselov, K. S. *Nat. Mater.* **2007**, *6*, 183.
(4) Li, Y. B.; Sinitskii, A.; Tour, J. M. *Nat. Mater.* **2008**, *7*, 966.
(5) Bunch, J. S.; van der Zande, A. M.; Verbridge, S. S.; Frank, I. W.; Tanenbaum, D. M.; Parpia, J. M.; Craighead, H. G.; McEuen, P. L. *Science* **2007**, *315*, 490.
(6) Nihar, M.; Vikas, B. *Nano Lett.* **2008**, *8*, 4469.
(7) Schedin, F.; Geim, A. K.; Morozov, S. V.; Hill, E. W.; Blake, P.; Katsnelson, M. I.; Novoselov, K. S. *Nat. Mater.* **2007**, *6*, 652.
(8) Ang, P. K.; Chen, W.; Wee, A. T. S.; Loh, K. P. *J. Am. Chem. Soc.* **2008**, *130*, 14392.
(9) Chen, F.; Xia, J. L.; Tao, N. J. *Nano Lett.* **2009**, *9*, 1621.
(10) Chen, F.; Xia, J. L.; Ferry, D. K.; Tao, N. J. *Nano Lett.* **2009**, *9*, ASAP.
(11) Forzani, E. S.; Lu, D. L.; Leright, M. J.; Aguilar, A. D.; Tsow, F.; Iglesias, R. A.; Zhang, Q.; Lu, J.; Li, J. H.; Tao, N. J. *J. Am. Chem. Soc.* **2009**, *131*, 1390.
(12) Silva, F.; Gornes, C.; Figueiredo, M.; Costa, R.; Martins, A.; Pereira, C. M. *J. Electroanal. Chem.* **2008**, *622*, 153.
(13) Albrecht, T.; Moth-Poulsen, K.; Christensen, J. B.; Hjelm, J.; Bjornholm, T.; Ulstrup, J. *J. Am. Chem. Soc.* **2006**, *128*, 6574.
(14) Alam, M. T.; Islam, M. M.; Okajima, T.; Ohsaka, T. *Electrochem. Commun.* **2007**, *9*, 2370.
(15) Xia, J. L.; Chen, F.; Li, J. H.; Tao, N. J. *Nat. Nanotechnol.* **2009**, in press.
(16) Fang, T.; Konar, A.; Xing, H. L.; Jena, D. *Appl. Phys. Lett.* **2007**, *91*, 092109.
(17) Das, A.; Pisana, S.; Chakraborty, B.; Piscanec, S.; Saha, S. K.; Waghmare, U. V.; Novoselov, K. S.; Krishnamurthy, H. R.; Geim, A. K.; Ferrari, A. C.; Sood, A. K. *Nat. Nanotechnol.* **2008**, *3*, 210.
(18) Tan, Y. W.; Zhang, Y.; Bolotin, K.; Zhao, Y.; Adam, S.; Hwang, E. H.; Das Sarma, S.; Stormer, H. L.; Kim, P. *Phys. Rev. Lett.* **2007**, *99*, 246803.
(19) Adam, S.; Hwang, E. H.; Galitski, V. M.; Das Sarma, S. *Proc. Natl. Acad. Sci. U.S.A.* **2007**, *104*, 18392.
(20) Bard, A. J.; Faulkner, L. R. *Electrochemical Methods: Fundamentals and Applications*, 2nd ed.; John Wiley & Sons, Inc.: 2001.
(21) Israelachvili, J. N. *Intermolecular and Surface Forces*, 2nd ed.; Academic Press: London, 1992.

JA9041862